Supporting information

High-yield Production of aromatics over $CuFeO_2$/hierarchical HZSM-5 via CO_2 Fischer-Tropsch Synthesis

Yang Cheng[a,#], Yong Chen[a,#], Shuxian Zhang[b], Xiaoting Wu[a], Chide Chen[a], Xin Shi[a], Ming Qing[b], Jifan Li[a,*], Chun-Ling Liu[a], Wen-Sheng Dong[a,*]

[a]*Key Laboratory of Applied Surface and Colloid Chemistry (SNNU), MOE, School of Chemistry and Chemical Engineering, Shaanxi Normal University, Xi'an 710062, Shaanxi, China*

[b]*Synfuels China Co., Ltd., Beijing, 101407, PR China*

Yang Cheng and Yong Chen are co-first authors of this article

*Corresponding authors. *E-mail:* lijifan@snnu.edu.cn (*Jifan Li*), wsdong@snnu.edu.cn (*Wen-Sheng Dong*).

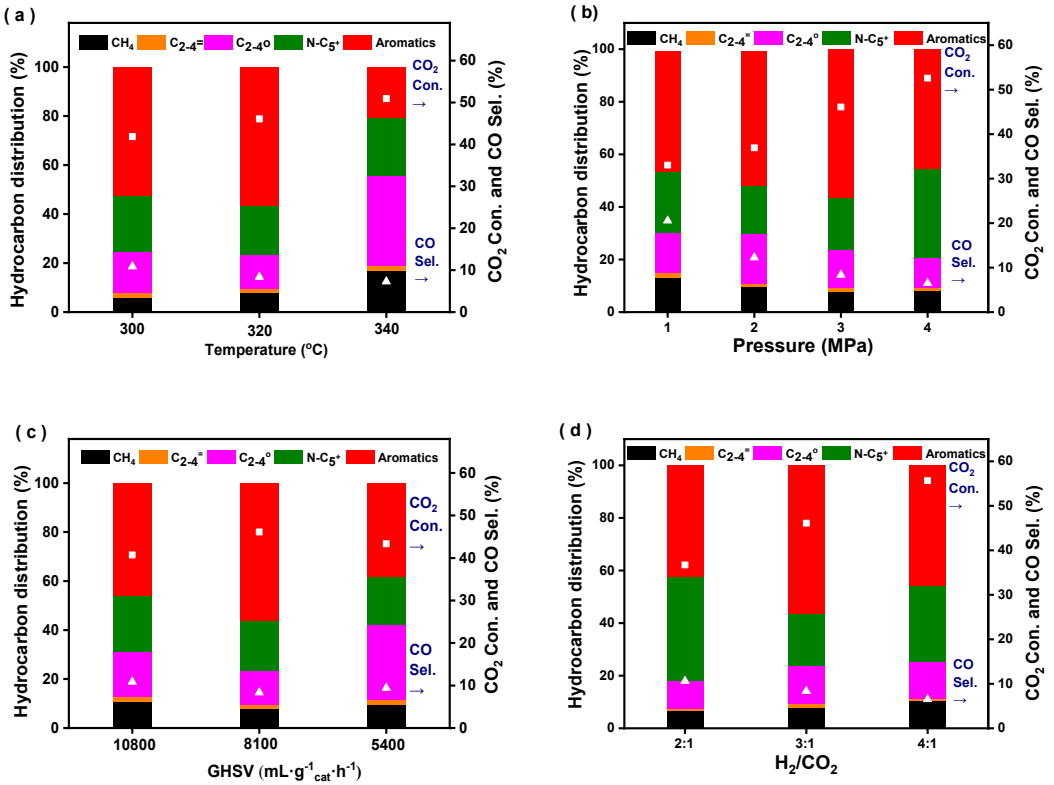

Fig. S1. The effects of reaction temperature (a), pressure (b), space velocity (c) and H_2/CO_2 ratio (d) on the catalytic performance over $CuFeO_2$/HZSM-5(*25*).

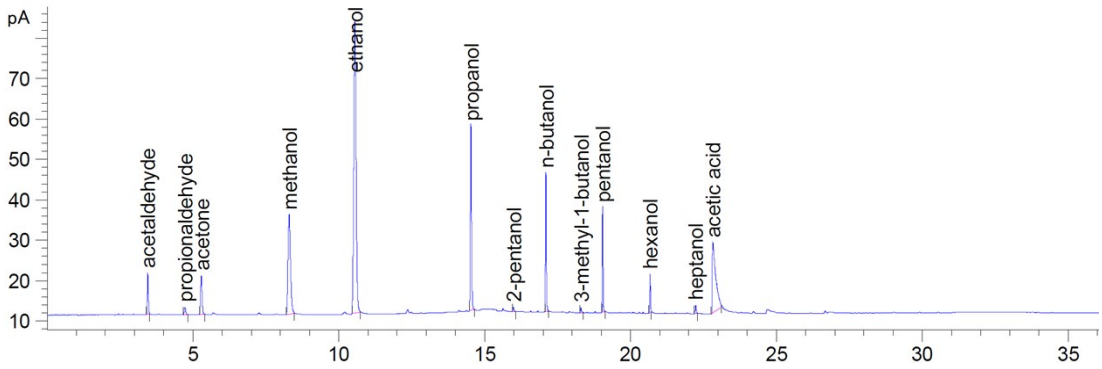

Fig. S2 Species in water phase obtained over $CuFeO_2$.

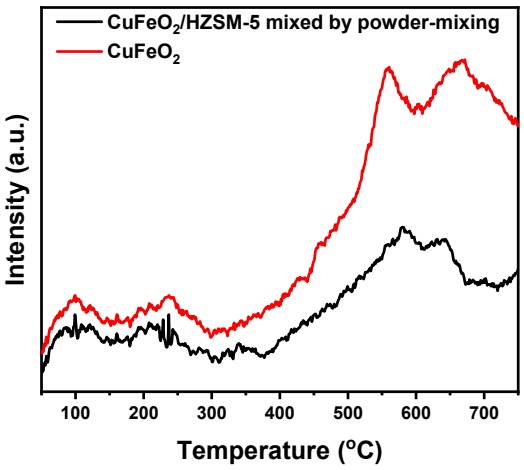

Fig. S3 The CO_2-TPD profiles of $CuFeO_2$ and $CuFeO_2$/HZSM-5(25) mixed by powder-mixing.

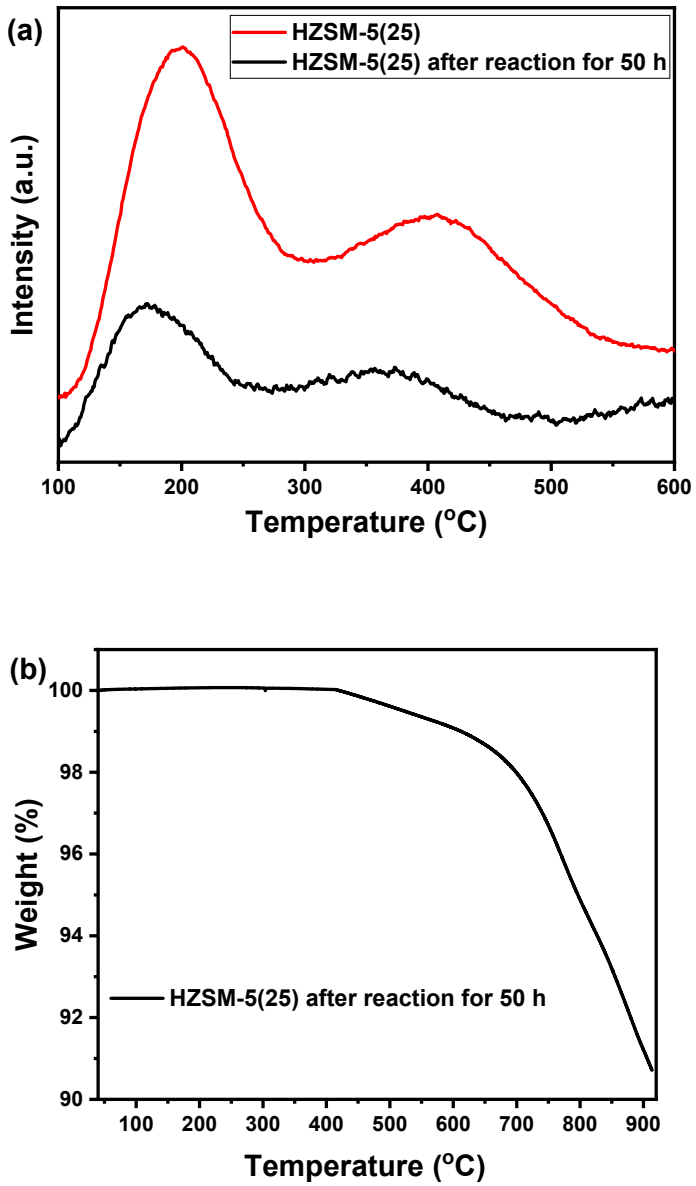

Fig. S4 The NH_3-TPD (a) and TGA (b) profiles of HZSM-5(*25*) after reaction for 50 h. (The carbon deposition on the spent HZSM-5(25) was determined by thermogravimetric analysis (TGA, HCT-4, China). Prior to the analysis, the spent sample was heat-treated under N_2 flow at a rate of 50 mL/min at 200 °C for 30 min in the TGA chamber. After the temperature of the TGA chamber decreased to 40 °C using a circulator, the TGA profiles were collected with increasing temperature till 900 °C at a heating rate of 5 °C/min under O_2 flow at a rate of 50 mL/min.)

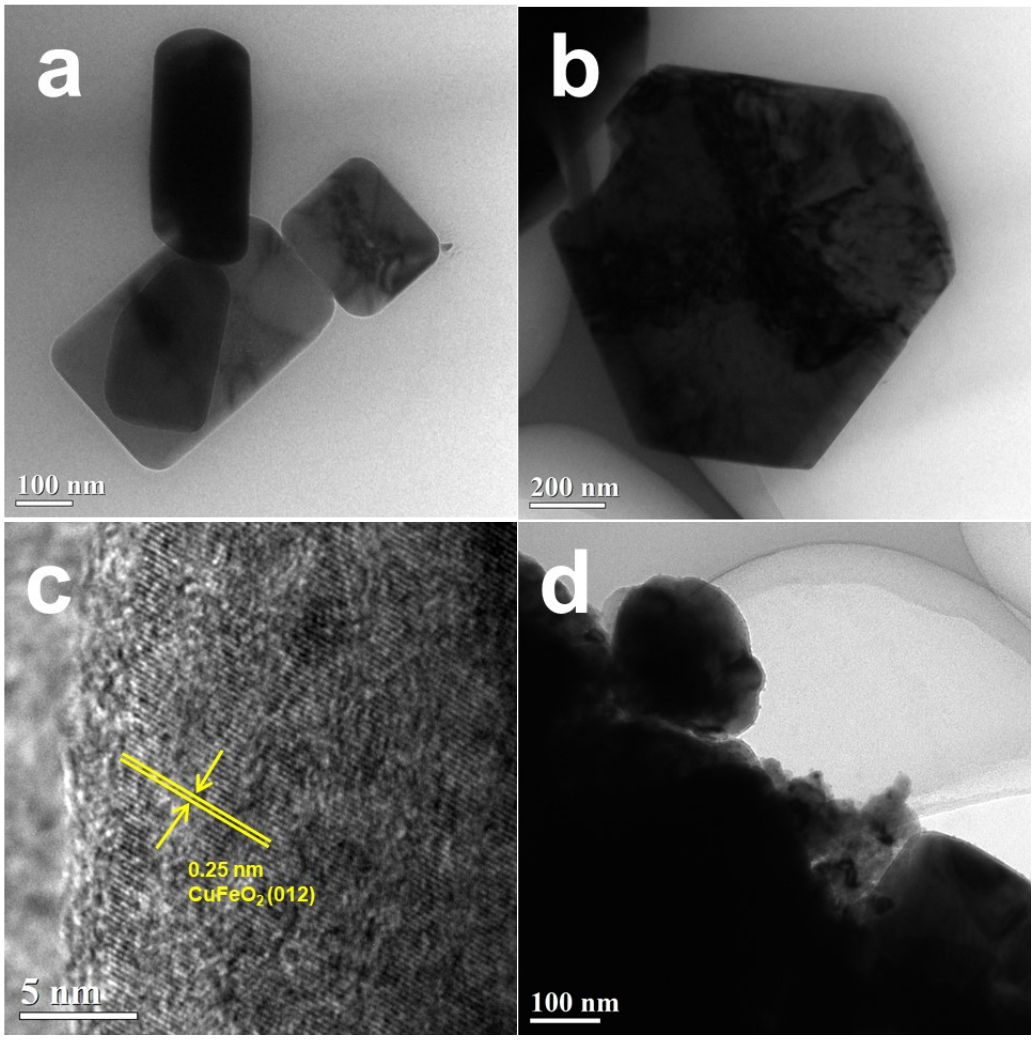

Fig. S5. TEM images (a-b) and HR-TEM image (c) of the fresh $CuFeO_2$, TEM image of the spent $CuFeO_2$ (d).

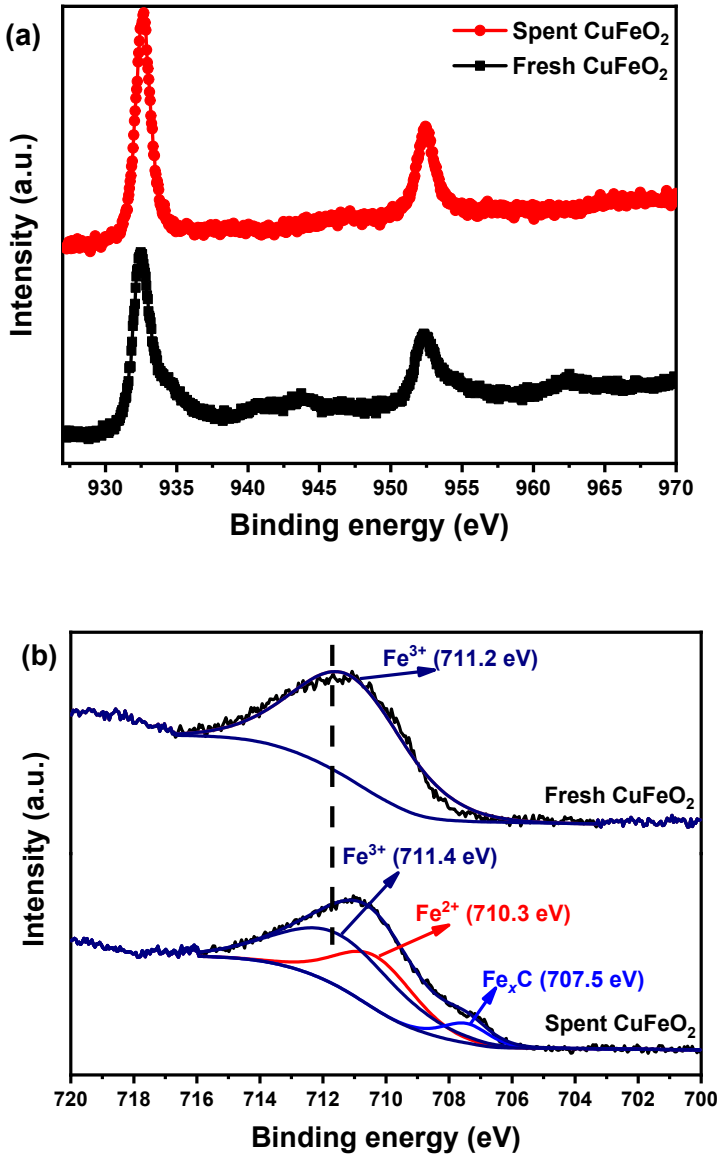

Fig. S6. Cu2p (a) and $Fe2p_{3/2}$ (b) XPS spectra of the fresh and spent $CuFeO_2$.

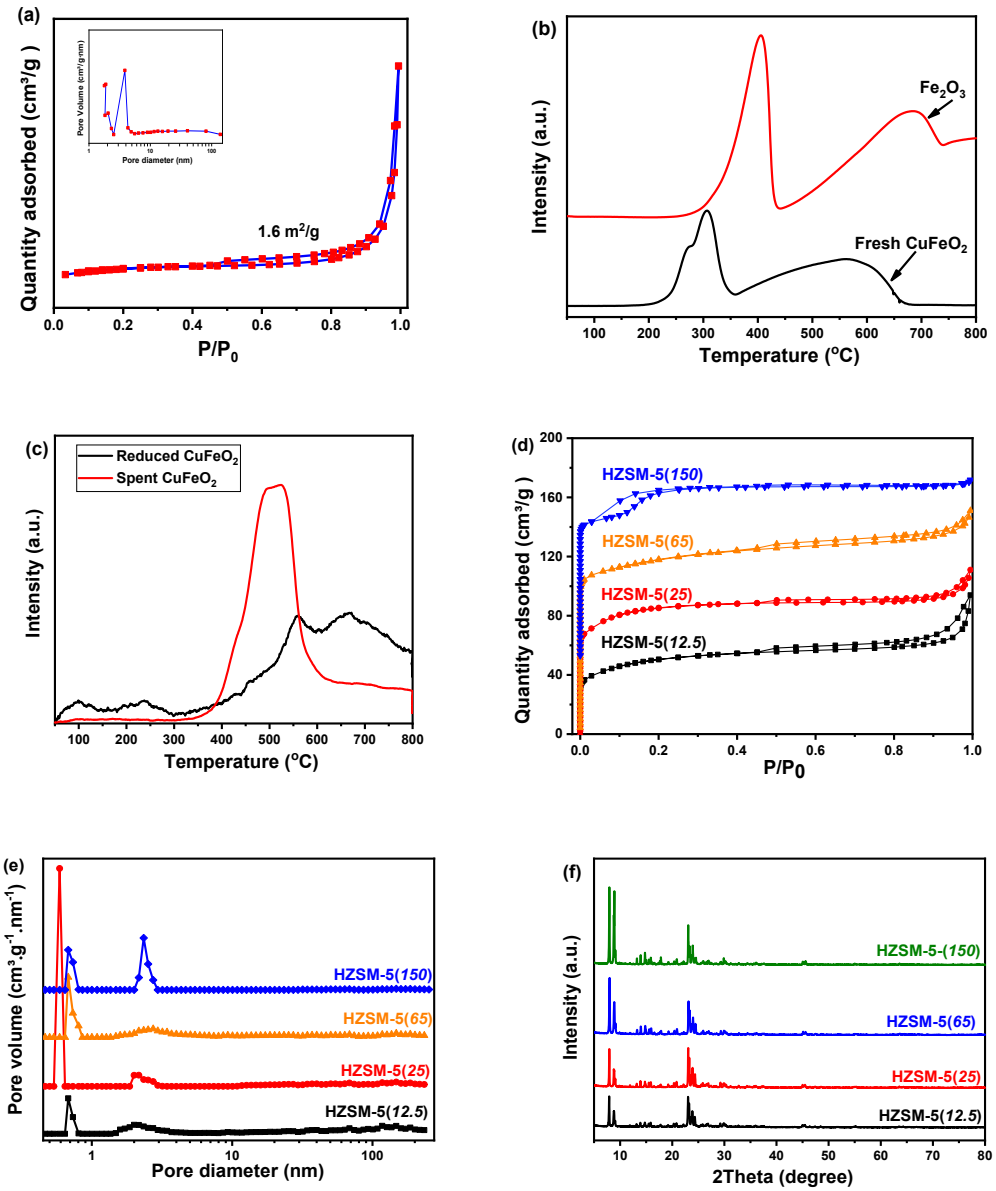

Fig. S7. N_2 adsorption-desorption isotherms and pore distribution of the fresh-$CuFeO_2$ (a), H_2-TPR profiles (b), CO_2-TPD profiles of the reduced and spent $CuFeO_2$, N_2 adsorption-desorption isotherms (d), pore distribution (e), and XRD patterns (f) of HZSM-5 with different Si/Al ratios.

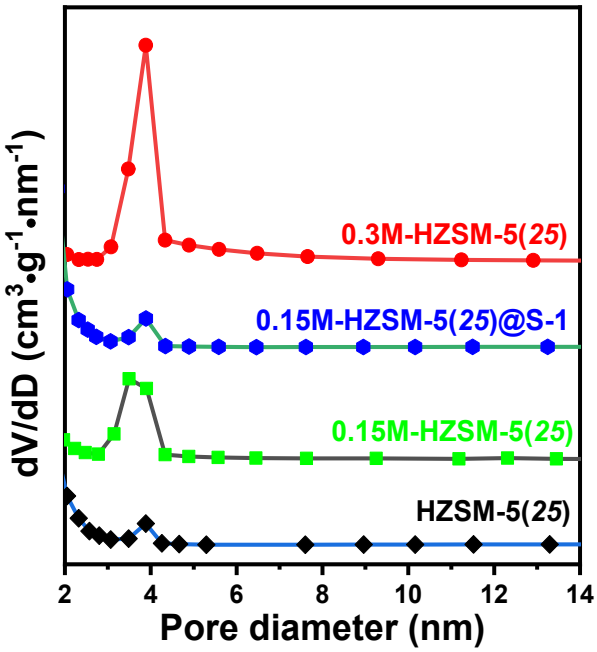

Fig. S8. Pore size distribution of different post treated HZSM-5(*25*)

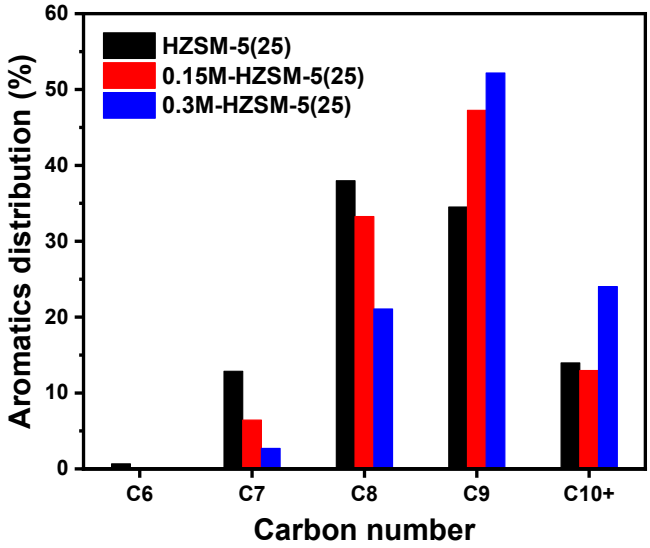

Fig. S9. Aromatics distribution of $CuFeO_2$ coupled with HZSM-5(*25*), 0.15M-HZSM-5(*25*) and 0.3M-HZSM-5(*25*). Reaction conditions: 320 °C, 3 MPa, $H_2/CO_2 = 3$, GHSV = 8100 $mL \cdot gcat^{-1} \cdot h^{-1}$ (The tabs of HZSM-5 represent the bifunctional catalysts of $CuFeO_2$ coupled with corresponding HZSM-5 in this figure).

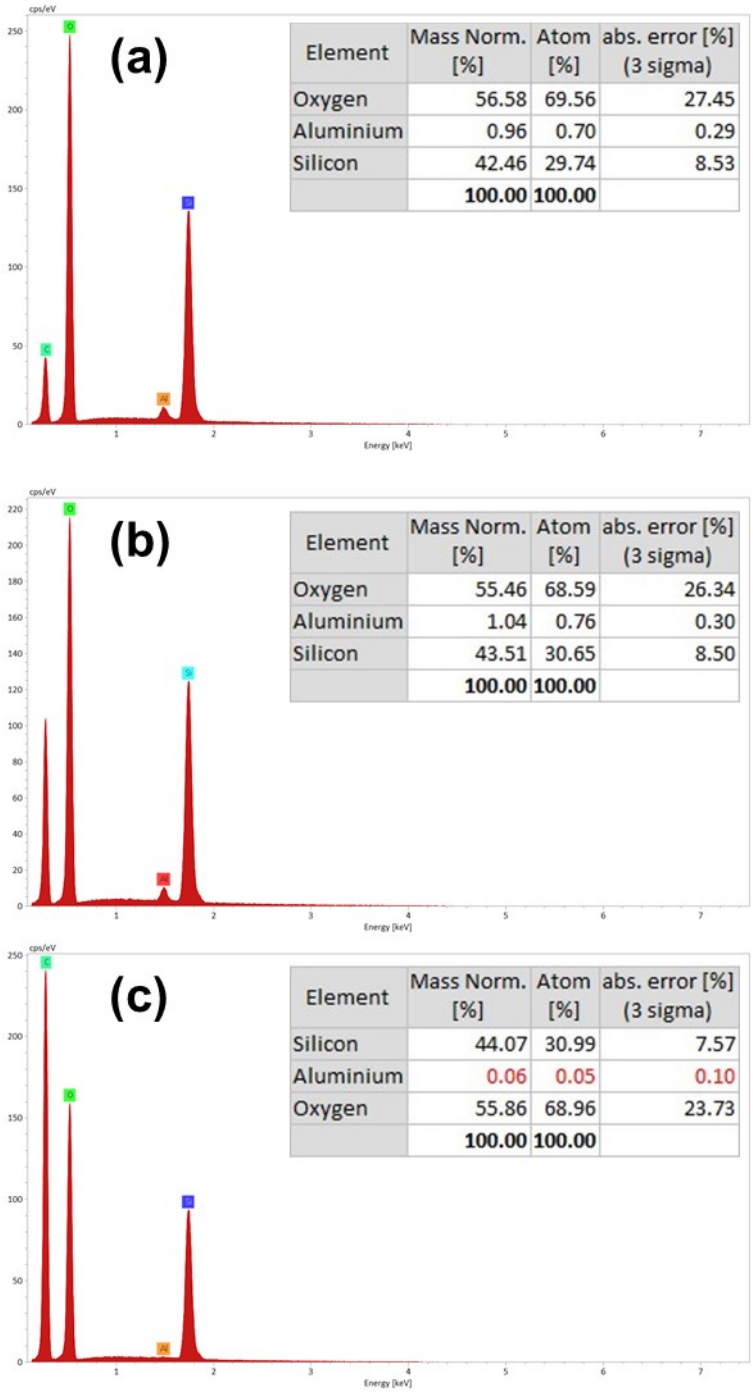

Fig. S10. Quantitative element analysis detected by EDS

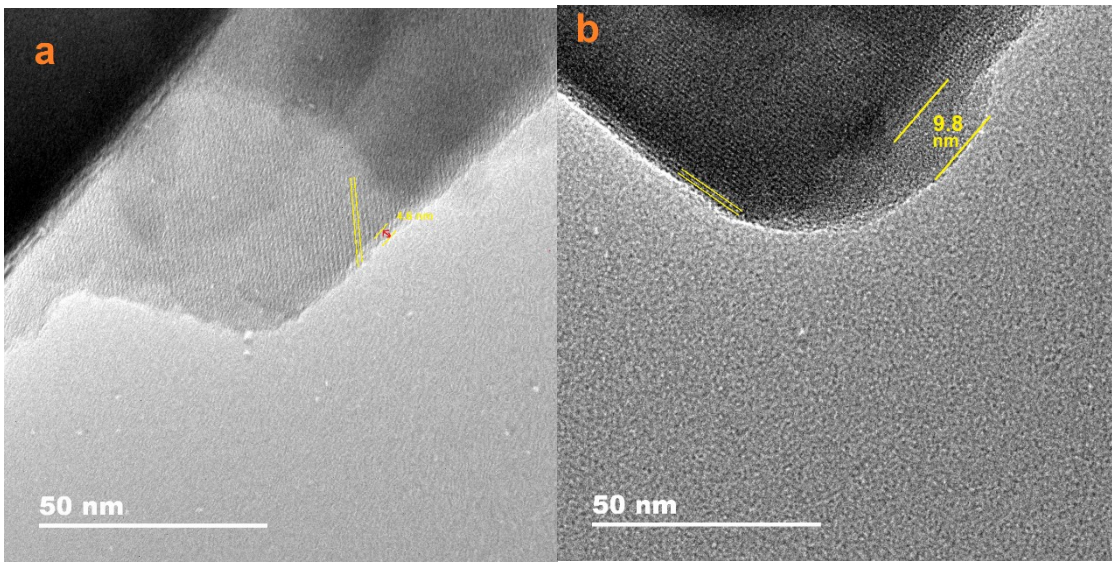

Fig. S11 The HRTEM images of the 0.15M-HZMS-5(25)@S-1.

Table S1 Comparison of catalytic performance

Entry Catalysts	Reaction conditions				CO_2 conv. (%)	CO sel. (%)	Hydrocarbon distribution (%)				Aro.STY	Ref.
	H_2/CO_2	T (℃)	P (MPa)	GHSV			CH_4	C_2-C_4	C_{5+} aliphatic	Aro.		
ZnZrO/HZSM-5	3	320	4	1200	14.1	44.0	0.4	19.6	7.0	73.0	10.6	1
ZnO-ZrO_2/HZSM-5(*300*)	3	340	3	2700	9.1	42.5	0.6			70.0	16.1	2
$ZnZrO_x$/HZSM-5	3	315	3	1020	17.5	23.8	1.2	29.8	7.7	60.3	12.6	3
$ZnAlO_x$/Si-HZSM-5	3	320	3	6000	5.0	47.0	1.0	29.5	2.5	67.0	16.6	4
Cr_2O_3/ZnZSM-5@Si-1	2.7	350	3	1200	22.1	35.1	4.5	22.6	2.8	70.1	18.9	5
$ZnCr_2O_4$/HZSM-5	3	350	4	1200	23.1	27.8	0.5	12.3	1.8	85.3	26.7	6
ae-Zn-ZrO_2/HZSM-5	3	340	4	2400	15.9	34	0.3	19.4	4.3	76.0	29.9	7
6.25Cu-Fe_2O_3/HZSM-5-pt	3	320	3	1000	55.4	4.4	12.5	9.4	15.4	61.9	51.2	8
Fe_2O_3@KO_2/ZSM-5	3	375	3	5000	48.9	12.8	13.9	45.9	15.3	24.9	82.9	9
$ZnFeO_x$-4.25Na/S-ZSM-5-Si	3	320	3	4000	36.9	11.1	9.7	27.7	21.6	41.0	83.9	10
Na-Fe_3O_4/HZSM-5(*25*)-Si-1x12%	2	320	3	4000	28.5	15	6.2	32.7	18.1	43.0	86.9	11
Na–$FeAlO_x$/Zn-HZSM-5(*12.5*)@SiO_2	3	370	3	4000	45.2	15.3	13.8	26.2	21.3	38.7	92.6	12
Na-Fe@C/0.2M-HZSM-5	3	320	3	9000	33.3	13.3	4.8	10.4	34.6	50.2	203.7	13
1.5KFe/HSG&HZSM-5(*50*)	3	340	2	26000	35.0	39.0	3.5	4.4	24.0	68.0	589.8	14
$CuFeO_2$/0.15M-HZSM-5(*25*)	3	320	3	8100	52.8	7.3	4.1	14.1	13.4	69.7	431.8	this work

1 Z. Li, Y. Qu, J. Wang, H. Liu, M. Li, S. Miao, C. Li, *Joule*, 2019, **3**, 570-583.

2 X. Zhang, A. Zhang, X. Jiang, J. Zhu, J. Liu, J. Li, G. Zhang, C. Song, X. Guo, *J. CO_2 Util.*, 2019, **29**, 140-145.

3 T. Wang, C. Yang, P. Gao, S. Zhou, S. Li, H. Wang, Y. Sun, *Appl. Catal. B-Environ.*, 2021, **286**, 119929.

4 Y. Ni, Z. Chen, Y. Fu, Y. Liu, W. Zhu, Z. Liu, *Nat. Commun.*, 2018, **9**, 3457.

5 Y. Wang, W. Gao, S. Kazumi, H. Li, G. Yang, N. Tsubaki, *Chem. Eur. J.*, 2019, **25**, 5149-5153.

6 W. Gao, L. Guo, Y. Cui, G. Yang, Y. He, C. Zeng, A. Taguchi, T. Abe, Q. Ma, Y. Yoneyama, N. Tsubaki, *ChemSusChem*, 2020, **13**, 6541-6545.

7 C. Zhou, J. Shi, W. Zhou, K. Cheng, Q. Zhang, J. Kang, Y. Wang, *ACS Catal.*, 2020, **10**, 302-310.

8 G. Song, M. Li, P. Yan, M.A. Nawaz, D. Liu, *ACS Catal.*, 2020, **10**, 11268-11279.

9 A. Ramirez, A. Dutta Chowdhury, A. Dokania, P. Cnudde, M. Caglayan, I. Yarulina, E. Abou-Hamad, L. Gevers, S. Ould-Chikh, K. De Wispelaere, V. van Speybroeck, J. Gascon, *ACS Catal.*, 2019, **9**, 6320-6334.

10 X. Cui, P. Gao, S. Li, C. Yang, Z. Liu, H. Wang, L. Zhong, Y. Sun, *ACS Catal.*, 2019, **9**, 3866-3876.

11 J. Wei, R. Yao, Q. Ge, D. Xu, C. Fang, J. Zhang, H. Xu, J. Sun, *Appl. Catal. B-Environ.*, 2021, **283**, 119648.

12 M.G. Sibi, M.K. Khan, D. Verma, W. Yoon, J. Kim, *Appl. Catal. B-Environ.*, 2022, **301**, 120813.

13 Y. Wang, S. Kazumi, W. Gao, X. Gao, H. Li, X. Guo, Y. Yoneyama, G. Yang, N. Tsubaki, *Appl. Catal. B-Environ.*, 2020, **269**, 118792.

14 S. Wang, T. Wu, J. Lin, J. Tian, Y. Ji, Y. Pei, S. Yan, M. Qiao, H. Xu, B. Zong, *ACS Sustain. Chem. Eng.*, 2019, **7**, 17825-17833.

Table S2 The element composition of fresh $CuFeO_2$ and Si/Al of different HZSM-5

Sample	Si/Al mol ratio[a]	Cu (mass%)[b]	Fe (mass%)	Na (mass%)
Fresh $CuFeO_2$		52.8	47.2	-[c]
HZSM-5(12.5)	15.7			
HZSM-5(25)	25.4			
HZSM-5(65)	66.1			
HZSM-5(150)	152.8			
0.15M-HZSM-5(25)	24.0			
0.3M-HZSM-5(25)	23.5			
0.15M-HZSM-5(25)@S-1	72.2			

[a]Determined by XRF

[b]Determined by ICP

[c]Not detected

Table S3 Catalytic performances of Fe_2O_3, $CuFeO_2$ and bifunctional catalysts[a]

Catalyst	CO_2 Conv. (%)	CO Sel. (%)	Hydrocarbon distribution (%)					o/p[d]
			CH_4	C_{2-4}^{o}	$C_{2-4}^{=}$	[b]N-C_5^+	Aromatics	
Fe_2O_3	19.6	18.8	28.7	17.2	9.6	44.5	-[c]	0.36
$CuFeO_2$	49.7	7.9	7.2	2.5	13.4	76.9	-[c]	4.77
HZSM-5(150)[e]	45.4	9.1	8.7	6.1	11.7	37.8	35.7	2.18
HZSM-5(65)[e]	47.9	8.3	8.6	8.6	4.8	31.7	46.3	0.61
HZSM-5(25)[e]	46.1	8.6	8.0	14.1	1.6	20.0	56.3	0.15
HZSM-5(12.5)[e]	45.0	8.7	10.2	17.7	1.7	23.4	47.0	0.11

[a]Reaction conditions: 320 ^oC, 3 MPa, H_2/CO_2 = 3, GHSV = 8100 $mL \cdot gcat^{-1} \cdot h^{-1}$.

[b]C_5^+ hydrocarbon excluded aromatics.

[c]Not detected.

[d]The ratio of olefins/alkane for C_{2-4}.

[e]Represented $CuFeO_2$ coupled with different HZSM-5.

Table S4 The Mössbauer parameters of the spent $CuFeO_2$

Catalyst	IS (mm/s)	QS (mm/s)	Area (%)	Assignment
Spent $CuFeO_2$	0.40	-0.02	23.39	Fe_3O_4 (A)
	0.70	-0.67	13.14	Fe_3O_4 (B)
	0.38	0.11	12.20	Fe_5C_2 (A)
	0.32	0.02	26.19	Fe_5C_2 (B)
	0.38	-0.02	13.15	Fe_5C_2 (C)
	0.40	0.18	8.06	Fe_3C (A)
	0.30	-0.04	3.86	Fe_3C (B)

Table S5 Catalytic performances of different $CuFeO_2$/HZSM-5(*25*) catalysts[a]

Catalyst	CO_2 Conv. (%)	FTY[b]	CO Sel. (%)	Hydrocarbon distribution (%)					o/p[d]
				CH_4	C_{2-4}^{o}	$C_{2-4}^{=}$	[c]N-C_5^+	Aromatics	
HZSM-5(*25*)[e]	46.1	3.1	8.6	8.0	14.1	1.6	20.0	56.3	0.15
0.15M-HZSM-5(*25*)[e]	52.8	3.6	7.3	4.1	12.5	1.6	13.4	69.7	0.16
0.3M-HZSM-5(*25*)[e]	40.9	2.8	10.2	4.2	7.3	4.7	12.7	71.9	0.58
0.15M-HZSM-5(*25*)@S-1[e]	45.2	3.1	11.7	6.2	9.4	10.3	19.7	54.4	1.04

[a]Reaction condition: 320 ^oC, 3 MPa, H_2/CO_2 = 3, GHSV = 8100 $mL \cdot gcat^{-1} \cdot h^{-1}$.

[b](FTY 10^{-5} mol of CO_2 converted per g of Fe in the catalyst per second)

[c]C_5^+ hydrocarbon excluded aromatics.

[d]The ratio of olefins/alkane for C_{2-4}.

[e]Represented $CuFeO_2$ coupled with different HZSM-5.